DOI: 10.1002/ejic.200900945

Mono- and Binuclear Arylnickel Complexes of the α-Diimine Bridging Ligand 2,2′-Bipyrimidine (bpym)

Axel Klein,*[a] Ann-Kathrin Schmieder,[a] Natascha Hurkes,[a] Claudia Hamacher,[a] Andreas O. Schüren,[a] Martin P. Feth,*[b] and Helmut Bertagnolli[b]

Keywords: Nickel / Electrochemistry / EPR spectroscopy / N ligands / Radical complexes / Spectroelectrochemistry

The mono- and binuclear organometallic Ni^{II} complexes [(μ-bpym){Ni(Mes)Br}$_n$] (bpym = 2,2′-bipyrimidine; n = 1 or 2; Mes = mesityl = 2,4,6-trimethylphenyl) were prepared and characterised electrochemically and spectroscopically (NMR, UV/Vis/NIR) in detail. The long-wavelength absorptions for the binuclear complex reveal a marked electronic coupling of the two metal centres over the ligand bridge via their low-lying π*-orbitals. While the mononuclear complex undergoes rapid dissociation of the bromido ligand after one-electron reduction the binuclear derivative exhibits reversible reductive electrochemistry and both of them yield stable radical anionic complexes with mainly bpym ligand centred spin density as shown by EPR spectroscopy of the free ligand bpym and the nickel complexes. The molecular structure of the binuclear bpym complex [(μ-bpym){Ni(Mes)Br}$_2$] was studied by EXAFS in comparison to the mononuclear analogue [(bpym)Ni(Mes)Br] revealing markedly increased Ni–C/N distance of the first coordination shell for the binuclear derivative suggesting an optimum overlap for the mononuclear complex, while two nickel complex fragments {Ni(Mes)Br} are seemingly too large to fit into the bis-chelate coordination site.

Introduction

Organometallic nickel complexes with α-diimine (diazene) ligands like 2,2′-bipyridine (bpy), 1,10-phenanthroline (phen) or diazabutadienes (R-DAB) have gained an enormous interest in the last decade. This is mainly due to a number of important catalytic processes like olefin oligo- or polymerization, olefin/CO co-polymerization,[1,2] and various (electro)catalytic C–C coupling reactions.[3–10] Paralleling their use in catalysis, fundamental studies on structures and electronic properties of organonickel complexes with α-diimines have been carried out.[9–17] We have contributed to this with the investigation of a number of organonickel complexes [(N^N)Ni(Mes)X] (N^N = α-diimine ligands, Mes = mesityl = 2,4,6-trimethylphenyl, X = halides) with various diimine ligands. Their strucures and reactivity towards ligand exchange reactions have been studied using X-ray diffraction and absorption spectroscopy,[13,14] their photophysics and photochemistry were explored by a combination of multiple spectroscopy and quantum chemical calculations,[13,15,16] and finally, their redox chemistry was investigated,[16,17] with respect to the application of such systems in electrocatalytical C–C coupling reactions.[6] From theses studies we have a clear picture of the crucial role of the diimine ligand in these complexes. The lowest unoccupied MOs are mainly ligand(π*) centred, with the consequences, that both the intense colours (long-wavelength absorption bands) and the relatively low first

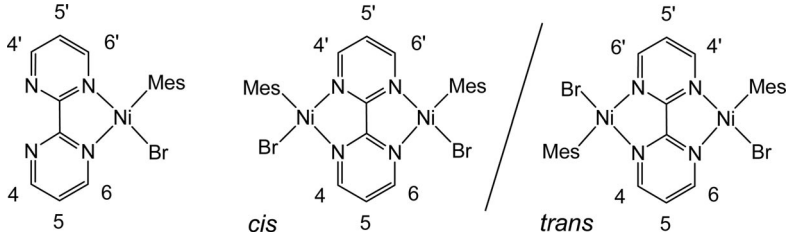

Scheme 1. Schematical drawing of the mononuclear complex [(bpym)Ni(Mes)Br] (left) and the two possible stereoisomers of the binuclear complex [(μ-bpym){Ni(Mes)Br}$_2$] (right) with partial numbering.

[a] Department für Chemie, Institut für Anorganische Chemie, Universität zu Köln,
Greinstraße 6, 50939 Köln, Germany
E-mail: axel.klein@uni-koeln.de
[b] Institut für Physikalische Chemie, Universität Stuttgart,
Pfaffenwaldring 55, 70569 Stuttgart, Germany
E-mail: martinphilipp.feth@sanofi-aventis.com

Supporting information for this article is available on the WWW under http://dx.doi.org/10.1002/ejic.200900945.

and second reduction potentials are strongly dependent on the nature of the diimine ligand.

These findings have promoted a study on the mono and binuclear complexes of the α-diimine (bis)chelate ligand 2,2′-bipyrimidine [(bpym){Ni(Mes)Br}$_n$] (n = 1 or 2; see Scheme 1), since we expected that the electronic coupling of two metal centres might greatly enhance these interesting properties.[18,19] In view of catalytical applications of such complexes binuclear derivatives are supposed to additionally offer higher thermal stability, as has been concluded in recent work e.g. by Jin and Huang.[2] The two metal atoms in complexes of bpym are oriented face to face with metal–metal distances of about 5.5–6 Å. This is too long for a direct metal–metal interaction, however the metals could interact via the low-lying lowest unoccupied molecular orbitals (LUMOs) of bpym.[19]

Results and Discussion

Synthesis and General Properties

The two neutral complexes [(bpym){Ni(Mes)Br}$_n$] (n = 1 or 2) were synthesised from the precursor complex *trans*-[$(PPh_3)_2$Ni(Mes)Br] by ligand exchange reactions in toluene solution and were analysed by ^{1}H NMR, ^{13}C NMR and elemental analysis (see Exp. Sect.). The stability of the two complexes was studied by recording the absorption spectra in various solvents to establish the solvatochromism of the long-wavelength absorption bands (see below). The two compounds are stable in solvents like CH_2Cl_2, THF, toluene, acetone and DMF towards ligand exchange reactions (dissociation of the bromido ligand).[14,16] In nitriles, DMSO and alcohols the complexes undergo the same decomposition reaction as reported for a number of monomolecular diimine complexes [(N^N)NiMesX] (N^N = various diimine ligands, X = halogenido).[14–16] This will be important for the further measurements in THF or DMF solutions (see below).

^{1}H NMR spectra revealed that the binuclear complex was obtained as 1.45 *trans*/1 *cis* mixtures of the two stereoisomers depicted in Scheme 1. Recrystallisation has no effect on the isomeric ratio. The complete spectral assignment of the isomers is given in the Experimental Section.

EXAFS Spectroscopy

Unfortunately, none of the two complexes could be obtained in form of single crystals. A suitable sample of the binuclear complex [(μ-bpym){Ni(Mes)Br}$_2$] was thus submitted to an EXAFS study. The data can be compared to the recently reported data of the mononuclear complex.[15]

Figure 1 illustrates the Ni-*K*-edge XANES spectra for [(bpym)Ni(Mes)Br] (complex **2d** in ref.[15]) and [(μ-bpym){Ni(Mes)Br}$_2$]. In both spectra the typical two pre-edge features, identifying square planar Ni^{II} complexes, can be observed.[20] The pre-peak at about 8333 eV can be assigned to a 1s→3d electron transition, while the second peak, which occurs at about 8337 eV, is due to a 1s→4p$_z$ transition with shakedown contributions.[21] Between both complexes clear differences in the Ni-XANES region can be found, indicating structural differences in the local environment of the absorbing nickel atoms of the complexes.

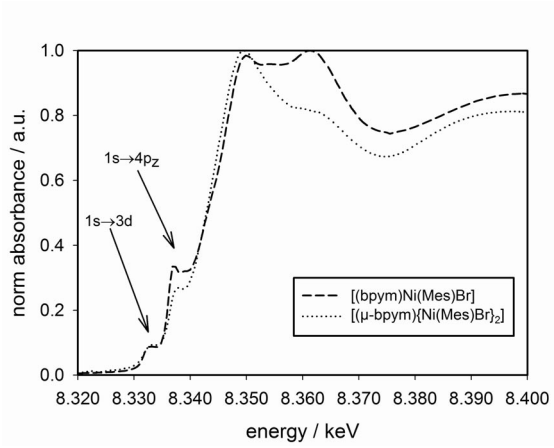

Figure 1. Comparison of the Ni-*K*-edge XANES spectra of [(bpym)-Ni(Mes)Br] and [(μ-bpym){Ni(Mes)Br}$_2$].

The fitting of the Ni-*K*-edge EXAFS spectra (Figure 2) of both investigated complexes was performed using a 3 shell model, in which the first coordination shell at about 1.9–2.0 Å consists of the two coordinating nitrogen atoms of the diimine ligand and the carbon atom of the mesityl group, the second shell of the bromine backscatterer at about 2.3 Å and the third coordination shell at about 2.8 Å of the further backbone-carbon-backscatterers of the mesityl and diimine ligand. Because of the nearly equal distances and backscatter behaviour of the nitrogen and carbon backscatterers in the first coordination shell, only one shell was fitted with nitrogen amplitude- and phase-functions. The Br-*K*-edge EXAFS spectra (Figure 3) were fitted with one coordination shell of nickel at ca. 2.3 Å.

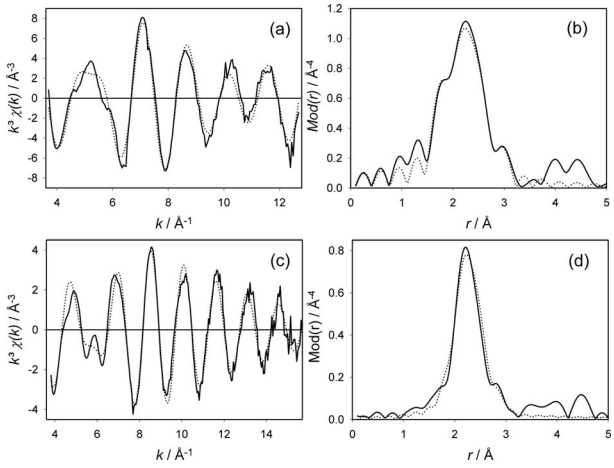

Figure 2. Experimental (solid line) and calculated (dotted line) k^3 $\chi(k)$ functions (a,c) and their Fourier transforms (b,d) of solid [(bpym)Ni(Mes)Br] (a,b) and [(μ-bpym){Ni(Mes)Br}$_2$] (c,d) at the Ni-*K*-edge.

Table 1. Structural parameter of the solid complexes determined from the Ni-*K*- and Br-*K*-edge EXAFS spectrum.

	[a]	r /Å	N	σ /Å	ΔE_0 /eV	k range /Å^{-1} (fit index, R)
[(bpym)Ni(Mes)Br]	Ni–C/N	1.91 ± 0.02	2.8 ± 0.3	0.056 ± 0.006	27.6	3.70–12.50
	Ni–Br	2.29 ± 0.02	1.2 ± 0.2	0.054 ± 0.008		(23.7)
	Ni–C	2.82 ± 0.03	2.8 ± 0.8	0.063 ± 0.019		
Complex **2d** in ref.[15]	Br–Ni	2.29 ± 0.02	0.9 ± 0.1	0.051 ± 0.007	13.5	4.00–12.50 (30.6)
[(μ-bpym){Ni(Mes)Br}$_2$]	Ni–C/N	2.03 ± 0.02	2.6 ± 0.3	0.097 ± 0.009	22.3	3.65–15.80
	Ni–Br	2.30 ± 0.02	0.8 ± 0.1	0.063 ± 0.009		(26.2)
	Ni–C	2.82 ± 0.03	1.7 ± 1.4	0.092 ± 0.027		
This work	Br–Ni	2.30 ± 0.02	1.0 ± 0.1	0.077 ± 0.008	15.7	3.70–15.00 (47.0)

[a] Absorber–backscatterer distance r, coordination number N, Debye–Waller factor σ with their calculated deviation, shift of the threshold energy ΔE_0 and the fit index R.

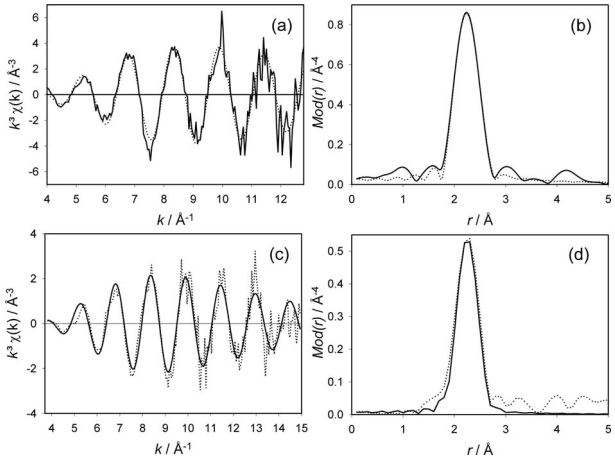

Figure 3. Experimental (solid line) and calculated (dotted line) k^3 $\chi(k)$ functions (a,c) and their Fourier transforms (b,d) of solid [(bpym)Ni(Mes)Br] (a,b) and [(μ-bpym){Ni(Mes)Br}$_2$] (c,d) at the Br-*K*-edge.

Structural parameters of the investigated complexes determined by curve fitting analyses of the EXAFS spectra at the Ni-*K*- and Br-*K*-edge are summarised in Table 1.

The results of the EXAFS analysis (distances, coordination numbers and Debye-Waller factors) at both edges of the binuclear complex are the average values for two nickel atoms present in the compound.

Significant structural differences between the mononuclear complex [(bpym)Ni(Mes)Br] and the binuclear derivative [(μ-bpym){Ni(Mes)Br}$_2$] were found from the analyses of the Ni-*K*-edge EXAFS spectra. In the binuclear complex the Ni–C/N distance of the first coordination shell is 0.12 Å longer than in the mononuclear species. This can be seen clearly in the Fourier transformed Ni-*K*-edge EXAFS spectrum of [(μ-bpym){Ni(Mes)Br}$_2$] (Figure 2), where the signals of the first (carbon and nitrogen backscatterers) and second (bromine backscatterer) coordination shells are no longer separated like in the Fourier transformed spectra of [(bpym)Ni(Mes)Br]. The Debye–Waller factor σ is also increased from 0.056 Å (N = 2.8) in the mononuclear compound to 0.097 Å (N = 2.6) in the binuclear complex. The increase in the Ni–C/N distance of the first coordination shell of the binuclear complex compared to the mononuclear derivative is probably due to the difficulties of the bpym bridging ligand to coordinate two metal atoms in an optimal way. For mononuclear complexes of bpym the bite angle N–Ni–N can be optimised for the metal and the ligand (preferably about 80°) by distorting the bpym ligand (enlargement of the N–C–C–N dihedral angle on the side of the metal) or by tilting the pyrimidine planes towards the coordination plane. For a binuclear complex only the latter option is principally available. However, for electronic reasons completely planar complexes were expected and indeed found.[19] Thus, as a last option to accommodate two metal atoms, the M–ligand distances increase. Such results were also reported earlier for similar binuclear complexes.[19]

The Br–Ni distance in both complexes remains constant in the order of magnitude, however its noteworthy to mention that the Debye-Waller factor of the coordination shell of bromine is increased for [(μ-bpym){Ni(Mes)Br}$_2$] compared with [(bpym)Ni(Mes)Br]. This might be due to two slightly different distances of Ni–Br in the binuclear compound in comparison with one Ni–Br distance in [(bpym)Ni(Mes)Br]. The Ni–C-distance of the third coordination shell remains constant in both complexes, whereas the coordination numbers decreases from ca. 3 in [(bpym)Ni(Mes)Br] to ca. 2 in [(μ-bpym){Ni(Mes)Br}$_2$].

Electrochemistry

The electrochemistry of the mononuclear complex has been described before.[17] The complex behaviour of the reduction waves can be explained with the rapid dissociation of the bromido ligand from the mono-reduced radical complex; see Equation (1).[17]

$$[(bpym)Ni(Mes)Br] + e^- \rightarrow [(bpym)Ni(Mes)Br]^{\cdot -} \rightarrow [(bpym)Ni(Mes)]^{\cdot} + Br^- \ (E + C) \quad (1)$$

The subsequently formed solvent complex [(bpym)Ni(Mes)(Solv)]$^{\cdot}$ undergoes further reductions. The presence of a solvent complex can be inferred from the marked dependence of the reduction potentials on the solvent (Table 2),

Table 2. Electrochemical data of the nickel complexes [(bpym){NiMesBr}$_n$] (n = 1 or 2).[a]

n	E_{pa} Ox2	E_{pa} Ox1	$E_{1/2}$ (ΔE_{pp}) or E_{pc} Red1	$E_{1/2}$ (ΔE_{pp}) or E_{pc} Red2	E_{pc} Red3	Solvent / T [°C]
1	–	0.31	–1.72 irr.	–2.10 irr.	–2.58	THF / 25
1	–	0.31	–1.58 irr.	–1.89 irr.	–2.32	DMF / 25
1	–	0.41	–1.53 (81)	–2.26 irr.	–	DMF / –60
2[b]	0.53	0.32	–1.12 (75)	–1.88 (92)[c]	–3.07	THF / 25
2[b]	0.50	0.30	–1.10 (84)	–1.85 irr.	–3.05	DMF / 25
2[b]	0.67	0.38	–1.11 (69)	–1.77 (78)	–3.00	DMF / –50

[a] Potentials from cyclic or square wave voltammetry in 0.1 M nBu$_4$NPF$_6$/solvent solutions (in V) vs. ferrocene/ferrocinium. Half wave potentials $E_{1/2}$ given with p*eak-to-peak* separation ΔE_{pp} in parentheses (in mV) for reversible processes; cathodic E_{pc}, or anodic E_{pa} peak potentials for irreversible processes. [b] The measurements were performed on a 1.45:1 *trans*/*cis* isomeric mixture. [c] The wave is only partly reversible with a current ratio I_{pa}/I_{pc} of 0.3.

however due to the irreversible nature of the waves these values are somewhat arbitrarily, since they also depend on the analyte concentration. At low temperature the first reduction occurs reversibly indicating, that the cleavage of the bromido ligand is retarded. The underlying mechanism of the bromide dissociation [Equation (1)] is the primarily diimine-centred reduction which is supported by spectroelectrochemistry[17] and in line with findings for related transitions metal complexes of bpym.[18,19] The second step is a more or less rapid cleavage of the bromido ligand as a result of partial transfer of the additional electron density to the metal. The latter idea is supported by findings on a series of mononuclear complexes [(N^N)Ni(Mes)Br], with diimine ligands (N^N) ranging from the rather basic but only weakly accepting ligand 3,4,7,8-tetramethyl-1,10-phenanthroline (tmphen) to the excellent acceptor 2,2′-bipyrazine (bpz). In this series the first reduction gained some reversibility with increasing acceptor capability of the diimine ligand. Indeed, E_1 for the bpym complex is partly reversible, while e.g. for the tmphen derivative the first reduction is completely irreversible.[17]

The electrochemistry of the binuclear complex exhibits a first reversible reduction wave and depending on the solvent a second irreversible (DMF) or partly reversible (THF) wave and all these waves occur at far higher (less negative) potentials compared to the mononuclear derivative. Following the explanations for the mononuclear complex,[17] the observed reversibility implies that the bromide dissociation is largely diminished for the binuclear complex if not completely inhibited. The reason lies in the coordination of a second metal ion (for the binuclear complex), which leads to the stabilisation of the ligand's LUMO,[19] thus leading to higher reduction potentials and to a decreased transfer of electron density from the reduced ligand (in the reduced complex) to the nickel atoms (which is the driving force for the Br dissociation).

On anodic scans broad irreversible oxidation waves were observed, which account for one electron for the mononuclear and two electrons for the binuclear complex. Based on similar results from mononuclear derivatives, we assign them to metal-centred oxidations Ni^{II}/Ni^{III} for the two nickel atoms.[16,17] From the wave of the binuclear complex it is not discernible if both nickel atoms are oxidised at the same potential (no electronic coupling), or if a mixed-valent state occurs (coupling of the metal centres).

Absorption Spectroscopy

The absorption spectra of both complexes (Figure 4) are dominated by two broad bands of medium intensity in the visible region and intense bands in the UV region. The two broad bands show negative solvatochromism, while the UV bands are solvent invariant. This was established be measurements in various solvent and correlation of the band energies to the E*MLCT solvent parameter established by Manuta and Lees for metal-to-ligand charge-transfer bands (for details see Supporting Information).[22]

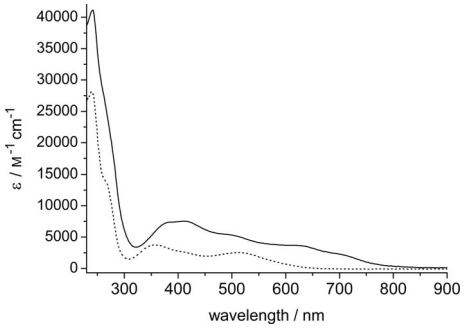

Figure 4. Absorption spectra of [(bpym)Ni(Mes)Br] (-----) and [(μ-bpym){Ni(Mes)Br}$_2$] (——) in CH_2Cl_2 solution.

Based on the band intensities, the observed solvatochromism and studies of related mononuclear complexes[14] we can assign the bands at high energy (band system I in Table 3) to ligand-centred (π-π*) transitions, while the two long-wavelength band systems (II and III) result from charge transfer transitions (mainly MLCT).

Table 3. Absorption maxima of parent nickel complexes [(bpym){Ni(Mes)Br}$_n$] (n = 1 or 2).[a]

	λ /nm		
n	I	II	III
1	*252* (28), 265 sh	*358* (3.8), 411 sh	494 sh, *511* (3.0)
2	*246* (42), 279 sh	391 sh, *414* (7.6)	483 sh, 567 sh, *624* (3.9), 690 sh

[a] Absorption maxima λ in nm as measured in CH_2Cl_2 solution, main maxima are in italics, extinction coefficients ε in 1000 $M^{-1}\,cm^{-1}$ are given in parentheses.

Comparison of the two complexes reveals that the two central bands shift from 358 and 511 nm (mononuclear) to 414 and 624 nm (binuclear) with markedly higher intensities

for the binuclear complex. This red-shift is commonly observed for related mono- and binuclear complexes of bpym and can be assigned to metal–metal coupling via the LUMO of the bridging ligand.[18,19]

EPR Spectroscopy

EPR spectra were recorded at ambient temperature from electrochemically generated radical anions of the two complexes. From the electrochemistry it can be expected that the reduced mononuclear complex $[(bpym)Ni(Mes)Br]^{\cdot-}$ will readily cleave the bromido ligand and the neutral species $[(bpym)Ni(Mes)(Solv)]^{\cdot}$ (Solv = THF or DMF) will be detected. In both solvents well resolved spectra were observed with hyperfine splitting (HFS) due to coupling to the ligands N and H atoms. The simulation of the spectra yielded spectral parameters (see Table 4), which are typical for transition metal complexes with a reduced bpym ligand.[19e,23,24] The spectral parameters of the species in DMF or THF solution are almost identical underlining that the influence of the solvent ligand in the detected species $[(bpym^{-})Ni^{II}(Mes)(Solv)]^{\cdot}$ is marginal. The binuclear complex $[(\mu\text{-bpym})\{Ni(Mes)Br\}_2]$ was also reduced in THF and DMF solution in which the first reductions occurs reversibly on the time scale of the CV experiment. Nevertheless, due to the long electrolysis time, partial bromide dissociation leading to $[Br(Mes)Ni(\mu\text{-bpym})Ni(Mes)(Solv)]^{\cdot}$ or $[(\mu\text{-bpym})\{Ni(Mes)(Solv)_2\}]^{\cdot+}$ cannot be excluded. In THF solution a well-resolved EPR spectrum (Figure 5), which was simulated with the values collected in Table 4 was observed (more figures are provided in the Supporting Information).

The coupling constants in the complexes are significantly increased compared to the free ligand. In the binuclear complex the values of the coupling are symmetrically distributed, whereas the mononuclear complex shows asymmetric distributed coupling constants. The same behaviour has been reported for related Cr^0 complexes,[19d,25] and strongly indicate that the singly occupied molecular orbitals (SOMOs) of the binuclear and the mononuclear species are mainly centred on the organic ligand. The observed increase of the coupling of the unpaired electron with the N atoms and the H4/H6 atoms of the ligand in the coordinated case are due to metal–ligand interaction. In contrast to this, in DMF solution only an ill-resolved spectrum was obtained, which could not be simulated. The two binuclear species exhibit markedly different g values and we can conclude different radical complexes to be responsible for the signals. It is reasonable to assume, that while in THF solution the complex remains coordinated by bromido coligands, in DMF we obtain solvated species under the electrolysis conditions.

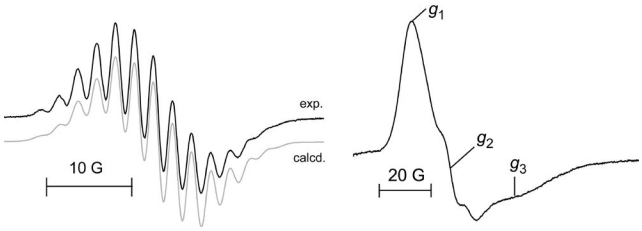

Figure 5. X-band EPR spectra of radical complexes generated from $[(\mu\text{-bpym})\{Ni(Mes)Br\}_2]$ in THF/nBu$_4$NPF$_6$ in situ electrolysis at 298 K and measured at 298 K (left, together with spectral simulation) and in glassy frozen solution at 110 K (right).

The g values of all radicals are quite close to those of $(bpym)^{\cdot-}$ (see Table 4), which strongly points to the bpym centred character of the radical complexes. A very suitable parameter to estimate the metal contribution is the g anisotropy (Δg), as measured from spectra at low temperature (in glassy frozen solutions).[17,18c] For the mononuclear and binuclear complexes Δg values ranging from 0.020 to 0.025 were obtained from unresolved spectra of rhombic symmetry (Figure 5 and Supporting Information), while the averaged g_{av} values are identical to the isotropic g values, testifying their identity. The absolute values of Δg indicate

Table 4. EPR data of radical anionic ligand $(bpym)^{\cdot-}$ and reduced (radical) complexes.[a]

Parent species	g_{iso}	a_{N1}	a_{N3}	a_{H4}	a_{H5}	a_{H6}	solvent
$[(\mu\text{-bpym})\{Ni(Mes)Br\}_2]$	2.0044	0.211	0.211	0.047	0.454	0.047	THF
$[(\mu\text{-bpym})\{Ni(Mes)Br\}_2]$	2.0025	_[b]	_[b]	_[b]	_[b]	_[b]	DMF
[(bpym)Ni(Mes)Br]	2.0038	0.239	0.192	0.038	0.446	0.045	THF
[(bpym)Ni(Mes)Br]	2.0038	0.239	0.192	0.038	0.452	0.045	DMF
bpym[c,d]	2.0030	0.143	0.143	0.015	0.492	0.015	THF
$[(\mu\text{-bpym})\{Cr(CO)_4\}_2]$[e]	2.0022	0.234	0.234	0.052	0.503	0.052	DMF
$[(bpym)Cr(CO)_4]$[e]	2.0022	0.239	0.152	0.024	0.500	0.057	DMF
$[(bpym)Cr(CO)_4]$[d]	2.0026	0.239	0.152	0.024	0.500	0.057	THF
	g_{av}[f]	g_1	g_2	g_3	Δg [f]		
$[(\mu\text{-bpym})\{Ni(Mes)Br\}_2]$	2.0044	2.0158	2.0066	1.9908	0.025		THF
$[(\mu\text{-bpym})\{Ni(Mes)Br\}_2]$	2.0025	2.0119	2.0041	1.9915	0.020		DMF
[(bpym)Ni(Mes)Br]	2.0037	2.0151	2.0049	1.9911	0.024		THF

[a] Generated in situ by electrolysis in THF or DMF with nBu$_4$NBF$_6$ as electrolyte and measured at 298 K; Isotropic g values g_{iso} and coupling constants a_X from spectral simulation (a_x in mT; 1 T = 10^4 G). [b] Simulation not possible due to bad spectral resolution (see text). [c] From ref.[24] [d] From ref.[25] [e] From ref.[19e] [f] Averaged g values $g_{av} = (g_1 + g_2 + g_3)/3$ and g anisotropy $\Delta g = g_1 - g_3$ obtained from measurements at 110 K in glassy frozen solutions.

rather low nickel contributions. Comparable values of 0.0165 and 0.018 have been obtained recently for the related species [(bpm)Ni(Mes)(Solv)]· (bpm = 4,4′-bipyrimidine) and [(bpy)Ni(Mes)$_2$]·, both of which are also clearly Ni^{II} complexes of reduced α-diimine ligands.[17] It is remarkable, that the binuclear species (measured in THF solution) exhibits an only slightly higher Δg than the mononuclear, although from simple considerations one would expect an approximately doubled value (two metal contributions instead of one). However, our EXAFS results have clearly shown that the ligand cannot accommodate two nickel atoms without lengthening the N–Ni bonds. This seems to be true also for the radical complexes. Thus, the individual contributions of the nickel atoms in the binuclear radical complex are far lower than the contribution by one nickel atom in the mononuclear complex and in summation they only slightly exceed the latter. Very similar results have been reported for reduced mono- and binuclear platinum(II) complexes of bpym.[19a,26]

Conclusions

Comparison of the mono and binuclear organometallic nickel complexes [(μ-bpym){Ni(Mes)Br}$_n$] (bpym = 2,2′-bipyrimidine; n = 1 or 2; Mes = mesityl = 2,4,6-trimethylphenyl) reveal a marked electronic coupling of the two metal centres over the ligand bridge via their low-lying π*-orbitals allowing the formation of one-electron reduced binuclear species [(μ-bpym$^-$){Ni^{II}(Mes)Br}$_2$]·$^-$, while the mononuclear derivative undergoes rapid dissociation of the bromido ligand yielding [(bpym$^-$)Ni^{II}(Mes)(Solv)]· Both radicals contain a mainly ligand-centred unpaired electron as evidenced from EPR spectroscopy. From the same method we can conclude, that the metal contribution is more or less the same for both radical complexes indicating a weaker metal-to-ligand interaction for the binuclear complex. This is not only true for the reduced species but also for the parent complexes as could be shown by EXAFS. Short Ni–N bonds providing an optimum orbital overlap, were found for the mononuclear complex, while two nickel complex fragments {Ni(Mes)Br} are seemingly too large to fit into the bis-chelate coordination site, which leads to prolonged Ni–N bonds and thus decreased metal-to-ligand overlap.

Experimental Section

Instrumentation: Elemental analysis was obtained using a HEKAtech CHNS EuroEA 3000 analyzer. NMR spectra were recorded on Bruker Avance II 300 MHz (^{1}H: 300.13 MHz, ^{13}C: 75.47 MHz) or Bruker Avance 400 MHz (^{1}H: 400.13 MHz, ^{13}C: 100.61 MHz) spectrometers, using a triple resonance ^{1}H,^{19}F,BB inverse probe head. The unambiguous assignment of the ^{1}H and ^{13}C resonances was obtained from ^{1}H TOCSY, ^{1}H COSY, gradient selected ^{1}H, ^{13}C HSQC and HMBC experiments. All 2D NMR experiments were performed using standard pulse sequences from the Bruker pulse program library. Chemical shifts were relative to TMS. Spectra were evaluated with Bruker TopSpin2. UV/Vis/NIR absorption spectra were recorded on Varian Cary 05E or Cary50 Scan spectrophotometers. Electrochemical experiments were carried out in 0.1 M nBu$_4$NPF$_6$ solutions using a three-electrode configuration (glassy carbon electrode, Pt counter electrode, Ag/AgCl reference) and an Autolab PGSTAT30 potentiostat and function generator. The ferrocene/ferrocenium couple served as internal reference. EPR spectra were recorded in the X band on the Bruker system ELEXSYS 500E, with a Bruker variable-temperature unit ER 4131VT. g values were calibrated by using a dpph sample. Spectral simulation was performed using Bruker Simphonia or PEST WinSim free software Version 0.96 (National Institute of Environmental Health Sciences).

EXAFS Measurements: The XANES and EXAFS measurements were performed at the beamlines X1.1 (RÖMO II) and E4 at the Hamburger Synchrotronstrahlungslabor des Deutschen Elektronen-Synchrotrons (HASYLAB at DESY, Hamburg, Germany), at beamline 2–3 at the Stanford Synchrotron Radiation Laboratory (SSRL) at SLAC (Stanford, USA) and at the newly designed EXAFS-beamline KMC-2 at the Berliner Elektronenspeicherring-Gesellschaft für Synchrotronstrahlung m.b.H (BESSY II, Berlin, Germany).

For the measurements at the Ni-K-edge (8332.8 eV) a Si(111) double crystal monochromator was used at the SSRL and at DESY. For the measurements at the Br-K-edge (13474.0 eV) at beamline X1.1 a Si(311) double crystal monochromator was used. At BESSY a SiGe(220) double graded-crystal (0.5% Ge/cm) monochromator was used for the nickel and the bromine edge. The synchrotron beam current was between 80–100 mA at HASYLAB (positron energy 4.45 GeV), between 100–250 mA at BESSY (electron energy 1.7 GeV) and between 80–100 mA at the SSRL (electron energy 1.7 GeV).

All experiments were carried out under ambient conditions at 25 °C. The tilt of the second monochromator crystal was set to 30% harmonic rejection. Energy resolution was estimated to be about 0.7–2.0 eV for the Ni-K-edge and 4.0 eV for the Br-K-edge. The spectra were collected in transmission mode with ion chambers. All ion chambers were filled with nitrogen in the case of the measurements at the Ni-K-edge, and the second and third chamber with argon in the case of the measurements at the Br-K-edge. Energy calibration was performed with the corresponding metal foils in the case of nickel and lead metal foil (Pb-L_{III}-edge) in the case of bromine. The solid complexes were embedded in a polyethylene matrix and pressed to pellets. The concentration of all samples was adjusted to yield an absorption jump of $\Delta\mu d \approx 1.5$.

Data evaluation started with background absorption removal from the experimental absorption spectrum by subtraction of a Victoreen-type polynomial. Then the background subtracted spectrum was convoluted with a series of increasingly broader Gauss functions and the common intersection point of the convoluted spectra was taken as energy E_0.[27] To determine the smooth part of the spectrum, corrected for pre-edge absorption, a piecewise polynomial was used. It was adjusted in such a way that the low-R components of the resulting Fourier transform were minimal. After division of the background subtracted spectrum by its smooth part, the photon energy was converted to photoelectron wave numbers k. The resulting EXAFS function was weighted with k^3 Data analysis in k space was performed according to the curved wave multiple scattering formalism of the program EXCURV92 with XALPHA phase and amplitude functions.[28] The mean free path of the scattered electrons was calculated from the imaginary part of the potential (VPI was set to –4.00) and an overall energy shift (ΔE_0) was

assumed. The Amplitude Reduction Factor (AFAC) was set to a value of 0.8 in the case of the Ni-*K*- as well as the Br-*K*-edge.

Materials and Procedures: The precursor complex [$(PPh_3)_2$Ni(Mes)Br][13,14] and the mononuclear complex [(bpym)Ni(Mes)Br][15] were obtained following literature procedures and analysed correctly. Other reagents were commercially available and used without further purification. All preparations and physical measurements were carried out in dried solvents under an argon atmosphere, using Schlenk techniques.

Synthesis of the Binuclear Complex μ-2,2′-Bipyrimidine-bis[bromomesitylnickel(II)] [(μ-bpym){Ni(Mes)Br}$_2$]: An amount of 72 mg of bpym (0.45 mmol) were added to 707 mg [$(PPh_3)_2$Ni(Mes)Br] (0.90 mmol) in 100 mL of toluene and stirred for three days after which the reaction mixture was dark brown. After evaporation to dryness, the residue was washed with three portions of 10 mL *n*-pentane and subsequently with three portions of 5 mL of acetone. From this acetone solution small amount of the mononuclear complex could be isolated. The residue was extracted with three portions of 20 mL of CH_2Cl_2 and the dark brown product was isolated from the combined filtrates by slow evaporation, standing overnight at 4 °C and subsequent filtering of the residue. After drying we obtained 236 mg (0.35 mmol, 78%) of a brown microcrystalline material. $C_{26}H_{28}Br_2N_4Ni_2$ (673.77): calcd. C 46.35, H 4.19, N 8.32; found C 46.23, H 4.17, N 8.33. ^{1}H NMR ([D$_6$]acetone): *cis* isomer: δ = 9.50 (d, ^3JH6′H5′ = ^3JH4′H5′ = 5.45 Hz, 2 H, H6′,4′), 8.24 (t, 1 H, H5′), 7.60 (t, ^3JH5H6 = ^3JH4H5 = 5.68 Hz, 1 H, H5), 7.30 (2 H, H4,6), 6.44 (s, 4 H, *m*-H), 3.01 (s, 12 H, *o*-CH_3), 2.16 (s, 6 H, *p*-CH_3); *trans* isomer: δ = 9.47 (dd, ^3JH6H5 = ^3JH4′H5′ = 5.39, ^4JH4′H6′ = 1.81 Hz, 2 H, H4′6), 7.92 (t, ^3JH6′H5′ = 5.72 Hz, 2 H, H5,5′), 7.35 (dd, ^4JH6H4 = 1.81 Hz, 2 H, H4,6′), 6.47 (s, 4 H, *m*-H), 3.02 (s, 12 H, *o*-CH_3), 2.19 (s, 6 H, *p*-CH_3) ppm.

Supporting Information (see also the footnote on the first page of this article): Absorption spectroscopic data of both complexes in various solvent (solvatochromism) together with plots of the long-wavelength absorption maximum (MLCT) with the E*MLCT solvent parameter. Also, cyclic voltammogramms and additional EPR spectra were provided.

Acknowledgments

We wish to thank HASYLAB at DESY (Hamburg, Germany), and BESSY II (Berlin, Germany) for the kind support of synchrotron radiation. C. H. and A. K. are grateful for support by the Deutsche Forschungsgemeinschaft (DFG KL 1194/5-1).

[1] a) B. Cornils, W. A. Herrmann (Eds.), *Applied Homogeneous Catalysis with Organometallic Compounds*, 2nd ed., Wiley-VCH, Weinheim, **2002**; b) S. D. Ittel, L. K. Johnson, M. Brookhart, *Chem. Rev.* **2000**, *100*, 1169–1203; c) A. Michalak, T. Ziegler, *Organometallics* **2001**, *20*, 1521–1532; d) S. Mecking, *Angew. Chem.* **2001**, *113*, 550–557; *Angew. Chem. Int. Ed.* **2001**, *40*, 534–540; e) V. C. Gibson, S. K. Spitzmesser, *Chem. Rev.* **2003**, *103*, 283–315; f) D. G. Yakhvarov, D. I. Tazeev, O. G. Sinyashin, G. Giambastiani, C. Bianchini, A. M. Segarra, P. Lönnecke, E. Hey-Hawkins, *Polyhedron* **2006**, *25*, 1607–1612; g) D. Meinhard, P. Reuter, B. Rieger, *Organometallics* **2007**, *26*, 751–754.

[2] a) Y.-B. Huang, G.-R. Tang, G.-Y. Jin, G.-X. Jin, *Organometallics* **2008**, *27*, 259–269; b) Q. Chen, J. Yu, J. Huang, *Organometallics* **2007**, *26*, 617–625.

[3] a) C. Moinet, J.-P. Hurvois, A. Jutand, *Adv. Org. Synth.* **2005**, *1*, 403–453; b) C. Amatore, A. Jutand, J. Périchon, Y. Rollin, *Monatsh. Chem.* **2000**, *131*, 1293–1304.

[4] a) J.-Y. Nédélec, J. Périchon, M. Troupel, *Top. Curr. Chem.* **1997**, *185*, 141–173; b) M. Durandetti, J. Périchon, *Synthesis* **2004**, 3079–3083; c) F. Raynal, R. Barhdadi, J. Périchon, A. Savall, M. Troupel, *Adv. Synth. Catal.* **2002**, *344*, 45–49.

[5] a) Y. H. Budnikova, *Russ. Chem. Rev.* **2002**, *71*, 111–139; b) D. G. Yakhvarov, Y. H. Budnikova, O. G. Sinyashin, *Russ. J. Electrochem.* **2003**, *39*, 1261–1269; c) D. G. Yakhvarov, Y. H. Budnikova, O. G. Sinyashin, *Mendeleev Commun.* **2002**, 175–176; d) Y. H. Budnikova, J. Périchon, D. G. Yakhvarov, Y. M. Kargin, O. G. Sinyashin, *J. Organomet. Chem.* **2001**, *630*, 185–192; e) Y. H. Budnikova, Y. M. Kargin, J.-Y. Nédélec, J. Périchon, *J. Organomet. Chem.* **1999**, *575*, 63–66.

[6] A. Klein, Y. H. Budnikova, O. G. Sinyashin, *J. Organomet. Chem.* **2007**, *692*, 3156–3167.

[7] a) J.-P. Corbet, G. Mignani, *Chem. Rev.* **2006**, *106*, 2651–2710; b) E. J. Anctil, G. V. Snieckus, in: *Metal-Catalyzed Cross-Coupling Reactions* (Eds.: A. de Meijere, F. Dieterich), Wiley-VCH, Weinheim, 2nd ed., **2004**, pp. 761–813.

[8] K. Tamao, *J. Organomet. Chem.* **2002**, *653*, 23–26.

[9] a) T. Yamamoto, *Synlett* **2003**, *4*, 425–450; b) K. Osakada, T. Yamamoto, *Coord. Chem. Rev.* **2000**, *198*, 379–399; c) T. Yamamoto, S. Wakabayashi, K. Osakada, *J. Organomet. Chem.* **1992**, *428*, 223–237.

[10] a) T. Yamamoto, M. Abla, Y. Murakami, *Bull. Chem. Soc. Jpn.* **2002**, *75*, 1997–2009; b) T. Yamamoto, M. Abla, *J. Organomet. Chem.* **1997**, *535*, 209–211; c) M. Uchino, K. Asagi, A. Yamamoto, S. Ikeda, *J. Organomet. Chem.* **1975**, *84*, 93–103; d) T. Yamamoto, A. Yamamoto, S. Ikeda, *J. Am. Chem. Soc.* **1971**, *93*, 3350–3359.

[11] a) G. C. Tucci, R. H. Holm, *J. Am. Chem. Soc.* **1995**, *117*, 6489–6496; b) A. Arcas, P. Royo, *Inorg. Chim. Acta* **1978**, *31*, 97–99; c) A. Arcas, P. Royo, *Inorg. Chim. Acta* **1978**, *30*, 205–207.

[12] R. F. De Souza, L. C. Simon, M. C. Alves, *J. Catal.* **2003**, *214*, 165–168.

[13] A. Klein, *Z. Anorg. Allg. Chem.* **2001**, *627*, 645–650.

[14] M. P. Feth, A. Klein, H. Bertagnolli, *Eur. J. Inorg. Chem.* **2003**, 839–852.

[15] M. P. Feth, A. Klein, H. Bertagnolli, S. Záliš, *Eur. J. Inorg. Chem.* **2004**, 2784–2796.

[16] A. Klein, A. Kaiser, W. Wielandt, F. Belaj, E. Wendel, H. Bertagnolli, S. Záliš, *Inorg. Chem.* **2008**, *47*, 11324–11333.

[17] A. Klein, A. Kaiser, B. Sarkar, M. Wanner, J. Fiedler, *Eur. J. Inorg. Chem.* **2007**, 965–976.

[18] a) W. Kaim, B. Sarkar, *Coord. Chem. Rev.* **2007**, *251*, 584–594; b) W. Kaim, T. Scheiring, M. Weber, J. Fiedler, *Z. Anorg. Allg. Chem.* **2004**, *630*, 1883–1893; c) A. Klein, *Rev. Inorg. Chem.* **2001**, *20*, 283–303.

[19] a) W. Kaim, A. Dogan, M. Wanner, A. Klein, I. Tiritiris, Th. Schleid, D. J. Stufkens, Th. L. Snoeck, E. J. L. McInnes, J. Fiedler, S. Záliš, *Inorg. Chem.* **2002**, *41*, 4139–4148; b) A. Klein, W. Kaim, F. M. Hornung, J. Fiedler, S. Záliš, *Inorg. Chim. Acta* **1997**, *264*, 269–278; c) M. Schwach, H.-D. Hausen, W. Kaim, *Chem. Eur. J.* **1996**, *2*, 446–451; d) W. Kaim, S. Kohlmann, *Inorg. Chem.* **1987**, *26*, 68–77; e) W. Kaim, *Inorg. Chem.* **1984**, *23*, 3365–3368.

[20] G. J. Colpas, M. J. Maroney, C. Bagyinka, M. Kumar, W. S. Willis, S. L. Suib, N. Baidya, P. K. Mascharak, *Inorg. Chem.* **1991**, *30*, 920–928.

[21] M. W. Renner, L. R. Furenlid, K. M. Barkigia, J. Fajer, *J. Phys. IV France* **1997**, *C2*, 661–662.

[22] D. M. Manuta, A. J. Lees, *Inorg. Chem.* **1983**, *22*, 3825–3828.

[23] S. Berger, A. Klein, W. Kaim, J. Fiedler, *Inorg. Chem.* **1998**, *37*, 5664–5671.

[24] M. Sieger, W. Kaim, D. J. Stufkens, T. L. Snoeck, H. Stoll, S. Záliš, *Dalton Trans.* **2004**, 3815–3821.

[25] W. Kaim, S. Ernst, *J. Phys. Chem.* **1986**, *90*, 5010–5014.

[26] A. Klein, E. J. L. McInnes, T. Scheiring, S. Zalis, *J. Chem. Soc. Faraday Trans.* **1998**, 2979–2984.
[27] a) T. S. Ertel, H. Bertagnolli, S. Hückmann, U. Kolb, D. Peter, *Appl. Spectrosc.* **1992**, *46*, 690–698; b) M. Newville, P. Livins, Y. Yakoby, J. J. Rehr, E. A. Stern, *Phys. Rev. B* **1993**, *47*, 14126–14131.
[28] S. J. Gurman, N. Binsted, I. Ross, *J. Phys. C* **1986**, *19*, 1845–1861.

Received: September 22, 2009
Published Online: January 12, 2010

